

# Synthesis, Characterization, and Ion Exchange Properties of Hydrotalcite $\text{Mg}_6\text{Al}_2(\text{OH})_{16}(\text{A})_x(\text{A}')_{2-x}\cdot 4\text{H}_2\text{O}$ ( $\text{A}, \text{A}' = \text{Cl}^-, \text{Br}^-, \text{I}^-, \text{and } \text{NO}_3^-, 2 \geq x \geq 0$ ) Derivatives

Ranko P. Bontchev, Shirley Liu, James L. Krumhansl, James Voigt, and Tina M. Nenoff\*

Sandia National Laboratories, P.O. Box 5800, MS 0734,  
Albuquerque, New Mexico 87185-0755

Received April 3, 2003. Revised Manuscript Received July 1, 2003

A series of monovalent anion-containing hydrotalcites (HTCs) with the general formula  $\text{Mg}_6\text{Al}_2(\text{OH})_{16}(\text{A})_x(\text{A}')_{2-x}\cdot 4\text{H}_2\text{O}$  ( $\text{A}, \text{A}' = \text{Cl}^-, \text{Br}^-, \text{I}^-, \text{and } \text{NO}_3^-, 2 \geq x \geq 0$ ) have been studied. Samples were synthesized by three different methods: ion exchange (IE), hydrothermal (HT), and recrystallization based on “memory effect” (ME). The physical, structural, and chemical characteristics and properties of the HTCs have been studied as a function of the synthetic methods and anions used. All three synthetic methods produced HTCs of good crystallinity and uniform particle size. When a second ( $\text{A}'$ ) or all four ( $\text{Cl}^-, \text{Br}^-, \text{I}^-, \text{NO}_3^-$ ) anions were present together with an  $\text{A}$ -HTC in an aqueous medium, the order of ion exchange preference was  $\text{Br}^- > \text{Cl}^- > \text{NO}_3^- > \text{I}^-$ . When using one-pot synthetic methods (HT, ME), the same order of anion incorporation preference,  $\text{Br}^- > \text{Cl}^- > \text{NO}_3^- > \text{I}^-$ , was observed.

## Introduction

Hydrotalcites (HTCs) are a large class of inorganic materials that have been extensively studied during the past decades because of their potential for practical applications in a wide variety of industrial and chemical processes. These include, but are not limited to, catalysis (catalysts, precursors, and supports), anionic exchange, electrodes, composite materials, etc.<sup>1–6</sup> Hydrotalcites are layered double-hydroxides with the general formula  $[\text{M}^{(\text{II})}_{1-x}\text{M}^{(\text{III})}_x(\text{OH})_2]^{x+}[\text{A}]_x\cdot m\text{H}_2\text{O}$  where  $\text{M}^{(\text{II})} = \text{Ca}^{2+}, \text{Mg}^{2+}, \text{Mn}^{2+}, \text{Fe}^{2+}, \text{Co}^{2+}, \text{Ni}^{2+}, \text{and } \text{Zn}^{2+}$ ;  $\text{M}^{(\text{III})} = \text{Al}^{3+}, \text{Cr}^{3+}, \text{Mn}^{3+}, \text{Fe}^{3+}, \text{Co}^{3+}, \text{and } \text{Ga}^{3+}$ ;  $\text{A} = \text{Cl}^-, \text{Br}^-, \text{I}^-, \text{NO}_3^-, \text{CO}_3^{2-}, \text{SO}_4^{2-}, \text{silicate-}, \text{polyoxometalate-}, \text{and/or organic anions}$ . For a recent review on synthetic HTCs see reference 7 and the references therein. The crystal structure of HTCs is closely related to that of the natural mineral brucite,  $\text{Mg}(\text{OH})_2$ ,<sup>8</sup> and is based on a stacking of hydroxide layers where part of the  $\text{M}^{(\text{II})}$  ions are substituted by  $\text{M}^{(\text{III})}$ . This replacement generates positively charged  $[\text{M}^{(\text{II})}/\text{M}^{(\text{III})}/\text{OH}]$  layers, which are compensated for by anions located between them. In the crystal structure, the positive and negative layers alternate along the  $c$ -direction of rhombohedral or hexagonal unit cells with typical lattice parameters of  $a_0 \sim 3.5 \text{ \AA}$  and  $c_0 \sim 22\text{--}25 \text{ \AA}$  (rhombohedral cell),

depending on the size of the anions involved.<sup>2,9–11</sup> The rhombohedral crystal structure, interlayer separation ( $L$ ), and unit cell of HTCs are illustrated in Figure 1.

A number of synthetic techniques have been successfully applied for the preparation of  $\text{M}^{(\text{II})}$ -,  $\text{M}^{(\text{III})}$ -, and  $\text{A}$ -substituted HTCs. The most common consists of a simple coprecipitation of dissolved  $\text{M}^{(\text{II})}/\text{M}^{(\text{III})}$  salts by a basic solution at pH values of about 10, typically using NaOH.<sup>1,12–17</sup> Variations of this method include the use of urea as both a carbonate source and a pH regulator,<sup>2</sup> a sol–gel synthesis using ethanol and acetone solutions,<sup>14</sup> and a fast nucleation process followed by a separate aging step at elevated temperatures.<sup>17</sup> In all of the above studies the synthesized HTCs contain only one type of anion. There is only one study where the precipitation synthesis of HTCs containing two anions,  $\text{CO}_3^{2-}$  and  $\text{SO}_4^{2-}$ , has been described.<sup>18</sup>

The second synthetic method is based on the so-called “memory effect”.<sup>4</sup> This term describes the following phenomenon. When heated above a certain temperature, the HTC's crystal structure collapses due to water and anions loss and the sample becomes amorphous. The anions are released as gases (as the corresponding

\* To whom correspondence should be addressed. Phone: (505)-844-0340. Fax: (505)-844-0968. E-mail: tmnenof@sandia.gov.

- (1) Miyata, S. *Clays Clay Miner.* **1975**, *23*, 369.
- (2) Constantino, U.; Marmottini, F.; Nocchetti, M.; Vivani, R. *Eur. J. Inorg. Chem.* **1998**, 1439.
- (3) Brindley, G. W.; Kikkawa, S. *Clays Clay Miner.* **1980**, *28*, 87.
- (4) Rey, F.; Fornes, V. J. *Chem. Soc. Faraday Trans.* **1992**, *88*, 2233.
- (5) Miyata, S. *Clays Clay Miner.* **1983**, *31*, 305.
- (6) Fogg, A. M.; Green, V. M.; Harvey, H. G.; O'Hare, D. O. *Adv. Mater.* **1999**, *11*, 1466.
- (7) Khan, I. A.; O'Hare, D. *J. Mater. Chem.* **2002**, *12*, 3191.
- (8) Zigan, F.; Rothbauer, R. *Neues Jahrb. Mineral. Monatsh.* **1967**, 137.

- (9) Allmann, R. *Acta Crystallogr., Sect. B* **1968**, *24*, 972.
- (10) Taylor, H. F. W. *Miner. Mag.* **1969**, *37*, 338.
- (11) Allmann, R. *Chimia* **1970**, *24*, 99.
- (12) Miyata, S.; Okada, A. *Clays Clay Miner.* **1975**, *25*, 14.
- (13) Aisawa, S.; Hirahara, H.; Uchiyama, H.; Takahashi, T.; Narita, E. *J. Solid State Chem.* **2002**, *167*, 152.
- (14) Aramendia, M. A.; Borau, V.; Jimenes, C.; Marinas, J. M.; Ruiz, J. R.; Urbano, F. J. *J. Solid State Chem.* **2002**, *168*, 156.
- (15) Newman, S. P.; Jones, W.; O'Connor, P.; Stamires, D. *J. Mater. Chem.* **2002**, *12*, 153.
- (16) Yun, S. K.; Pinnavaia, T. J. *Chem. Mater.* **1995**, *7*, 348.
- (17) Zhao, Y.; Li, F.; Zhang, R.; Evans, D. G.; Duan, X. *Chem. Mater.* **2002**, *14*, 4286.
- (18) Le Bail, C.; Thomassin, J.-H.; Touray, J. C. *Phys. Chem. Miner.* **1987**, *14*, 377.

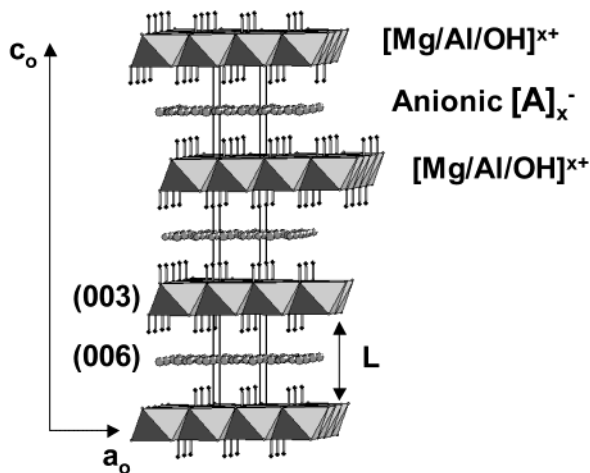


**Figure 1.** Representation of the HTC structure, cell parameters, characteristic charged layers (planes), and interlayer separation  $L$ .

$H_xA$  acids) while the  $[M^{(II)}/M^{(III)}/OH]$  layers remain relatively intact. After cooling to room temperature and immersion of the solid residue in an aqueous solution containing either the original or a different anion, the overall crystal structure recovers (the material “remembers” its initial structure) and the resulting product is again a crystalline HTC with alternating anionic and  $[M^{(II)}/M^{(III)}/OH]$  layers. This method has been successfully applied for the synthesis of  $I^-$ ,  $ReO_4^-$ , and mixed  $I^-/ReO_4^-$  HTCs.<sup>19,20</sup>

The last method for preparing HTCs is based on the classic ion exchange process. In this procedure, a synthesized A-HTC is dispersed in a water solution containing a second anion,  $A'$ . With time, the  $A'$  anions permeate the A-HTC matrix and partially substitute for A, forming a mixed  $A_xA'_{1-x}$ -HTC. A series of such double HTC has been prepared using  $Cl^-$ ,  $NO_3^-$ , and  $SO_4^{2-}$ -HTC matrixes and  $OH^-$ ,  $F^-$ ,  $Cl^-$ ,  $Br^-$ ,  $I^-$ ,  $NO_3^-$ ,  $CO_3^{2-}$ , and  $SO_4^{2-}$  containing solutions.<sup>5,19,20</sup>

The goal of our study was to investigate in a systematic way the relations between the synthetic method used and the ion exchange capacity of a series of monovalent anionic HTCs. The changes of the cell parameters and interlayer distances as a function of the chemical composition have also been studied. The morphology, particle size distribution, and surface area of the synthesized HTCs have been determined. Finally, the samples were also characterized by chemical and thermogravimetric analyses and FTIR spectroscopy.

## Experimental Section

**Synthesis.** Several series of individual and mixed HTCs with composition  $Mg_xAl_{2-x}(OH)_{16}(A_x)(A')_{2-x}\cdot 4H_2O$  ( $A, A' = Cl^-, Br^-, I^-, \text{ and } NO_3^-$ ,  $2 \geq x \geq 0$ ) have been prepared using three different synthetic methods.

**Hydrothermal Synthesis (HT).** One-pot hydrothermal reactions were carried out aiming at single anion A-HTCs. In a typical reaction, 0.769 g of  $Mg(NO_3)_2\cdot 6H_2O$  and 0.375 g of  $Al(NO_3)_3\cdot 9H_2O$  were dissolved in 4 mL of  $H_2O$ . A water solution of  $NH_4OH$  was then added dropwise with stirring until the pH reached a value of 8.5. At this point, a precipitation of Mg/

Al hydroxides took place and the solution changed to a milk-like suspension. The latter was transferred into a 23-mL Teflon-lined Parr reactor and heated for 24 h at 120 °C. The product, a finely dispersed white powder, was an XRD-pure  $NO_3^-$ -HTC, yield 98%.

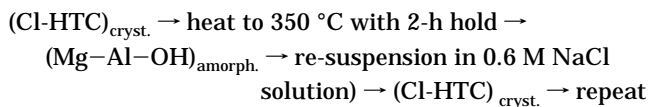
To determine the preference of anionic incorporation,  $ClA'$ - and  $NO_3A'$ -HTCs were synthesized using two different starting  $A/A'$  ratios of 1:1 and 1:3 ( $A = Cl, NO_3$ ;  $A' = Cl, Br, I, NO_3$ ) and the corresponding Mg- and Al-sources. An additional one-pot hydrothermal synthesis was carried out when the same amounts (2 mL) of all four anions ( $Cl^-$ ,  $Br^-$ ,  $I^-$ , and  $NO_3^-$ ) were present in equimolar (1 M) concentrations.

**Ion Exchange (IE).** Two sets of experiments were carried out. In the first series the simple binary  $A' \rightarrow A$  exchange properties of twelve pairs of  $(A\text{-HTC})_{\text{solid}}/(A')_{\text{soln}}$  ( $A, A' = Cl, Br, I, \text{ and } NO_3$ ) systems were studied. In all these experiments 0.5 g of each synthesized (HT) A-HTC were immersed in 6 mL of 1 M water solution of  $NaA'$  and stirred in closed vials at room temperature for 12 h. After the solutions were filtered, washed, and dried under vacuum, weighed amounts of the solid residues were dissolved in diluted  $H_2SO_4$  and the Cl, Br, I, and  $NO_3$  concentrations were determined by ion chromatography.

The second set of experiments was aimed at determining the ion exchange preferences when all four anions were present. Four different  $(A\text{-HTC})_{\text{solid}}/\Sigma(NaA')_{\text{soln}}$  systems were studied. In these experiments 0.5 g of each synthesized (HT) A-HTC were immersed in 6 mL of water solution consisting of 2 mL of equimolar (1 M) solutions of each  $NaA'$  ( $A, A' = Cl, Br, I, \text{ and } NO_3$ ). For example, solid Cl-HTC was immersed in 6 mL of solution made by mixing 2 mL of 1 M NaBr, 2 mL of 1 M NaI, and 2 mL of 1 M  $NaNO_3$ . The samples were stirred in closed vials for 12 h at room temperature, filtered, washed with deionized water, and dried in a drybox. Weighed amounts of the solid residues were dissolved in diluted  $H_2SO_4$ , and the Cl, Br, I, and  $NO_3$  concentrations were determined by IC.

**Memory Effect (ME).** The goal of these experiments was to explore the possibility of cross-synthesis, i.e., starting from A-HTC to prepare  $A'$ -HTC using the “memory effect”. For that purpose all synthesized (HT) A-HTCs ( $A = Cl^-, Br^-, I^-, NO_3^-$ ) were calcined at 350 °C for 2 h, after which they were suspended in solutions containing each of the other anions. In a typical reaction, 0.5 g of Cl-HTC was heated for 2 h at 350 °C in air. After cooling, the XRD amorphous residue was suspended in 6 mL of 1.0 M water solution of NaBr and left stirring overnight at room temperature. After the solution was washed and filtered, the resulting product was an XRD-pure Br-HTC, yield 96%.

Another series of experiments aimed to evaluate the effect of repeated (amorphous  $Mg-Al-OH$ )  $\rightarrow$  (crystalline A-HTC) cycles on the crystallinity and yield of the products. To determine the recycle potential, 10 consecutive cycles using Cl-HTC were performed according to the following scheme:



The crystallinity of the products was analyzed and compared after each cycle based on the relative intensity and HRFM of the corresponding 003 and 006 reflections in the powder X-ray diffraction patterns.

**Characterization.** *X-ray diffraction (XRD).* The HTC's phase purity, crystallinity, and cell parameters were determined by powder X-ray diffraction methods using a Siemens Kristalloflex D 500 diffractometer with monochromatized  $Cu\ K\alpha$  radiation. The degree of crystallinity of the different HTC preparations was evaluated and compared using the intensity and sharpness (HWF) of the corresponding 003 and 006 reflections. The  $c_0$ -cell parameters were determined with accuracy of  $\pm 0.005\text{ \AA}$  as the average of the  $c_0$ -values calculated based on the 003 and 006 reflections after profile fitting using the Jade 6.0 XRD software. The interlayer  $Mg/Al/OH-Mg/Al/OH$  separation  $L$  [ $\text{\AA}$ ] corresponds to the closest separation

(19) Fetter, G.; Ramos, E.; Olguin, M. T.; Bosch, P.; Lopez, T.; Bulbulian, S. *J. Radioanal. Nucl. Chem.* **1997**, *221*, 63.

(20) Kang, M. J.; Chun, K. S.; Rhee, S. W.; Do, Y. *Radiochim. Acta* **1999**, *85*, 57.

between the oxygen atoms of two adjacent layers. It was calculated as the shortest (center to center) O–O distance between oxygen atoms belonging to two adjacent Mg/Al/OH–Mg/Al/OH layers (typically located above each other along the *c*-axis), minus twice the ionic radius of  $O^{2-}$ .<sup>21</sup>

**Morphology, Surface Area and Particle Size Distribution.** Crystallite morphology was studied by scanning electron microscopy (SEM) using a Hitachi S4500 Field Emitter Gun (FEG) scanning electron microscope. The images were acquired digitally using Princeton Gamma Tech (PGT) acquisition hardware with Imix software. The powders were sprinkled on carbon tape and coated with AuPd for analysis. The surface area of the samples was determined using a Micromeritics ASAP (accelerated surface area and porosimetry system) 2010. The samples were degassed at 90 °C prior to analysis and analyzed using the multi-point method (5 points used). Powder particle size distributions were determined using a Coulter LS230 (Beckman Coulter) instrument using laser light with a wavelength of 750 nm. Two series of samples have been measured. In the first one the samples have been studied “as-synthesized”, i.e., after filtration and washing with deionized water the “wet” samples were rapidly transferred to the Coulter LS230 and measured. In the second series, the “wet” samples were first dried in a drybox under dynamic vacuum at room temperature and then characterized (SEM, surface area, and particle size distribution).

**FTIR and TGA.** Infrared spectra were collected using a Perkin-Elmer FTIR Spectrometer GX and KBr pellets for sample preparation. Thermogravimetric analyses were carried out in air using a TA Instruments at a heating rate of 2°/min.

**Chemical Analyses.** The anionic content of the solid HTC (after being dissolved in  $H_2SO_4$ ) and that of the solutions after ion exchange have been determined using a Dionex ion chromatograph (IC). Commercially available IC standards (Fischer Scientific) were used for the calibration curves for  $Cl^-$ ,  $Br^-$ ,  $I^-$ , and  $NO_3^-$ . Six experimental points within the range of 1–100 ppm for each anion were fitted by the least-squares method. In all cases a linear dependence of the integrated intensity as a function of the anionic concentration was obtained with correlation coefficients  $R_{Ai} = 0.993$  or better.

## Results and Discussion

**Synthesis. Ion Exchange.** The ion-exchange experiments showed that neither the type nor the number of anions involved produces a measurable change in the crystallinity of the resulting HTCs. The most important observation for this series, however, was that it is not possible to synthesize a single-anion A-HTC using this method at room temperature. In all experiments the final products contained at least two anions in comparable concentrations, i.e., it is not possible to achieve 100% ion exchange (see further in the text).

**Memory Effect.** The “memory effect”-based syntheses produced HTCs of inferior crystallinity compared to the samples prepared by the hydrothermal method as determined by XRD. However, the crystallinity could be significantly improved if the last stage — conversion of the amorphous Mg–Al–OH residue by suspension in the desired NaA solution — is carried out in a Parr reactor at  $T \geq 90$  °C for just 2 h. After 10 crystalline/amorphous cycles the final products were still well crystallized HTCs recovered in high (>90%) yields, although the crystallinity slightly decreased with the number of cycles. Our results also showed that all anions are absorbed completely reversibly and any anion can be exchanged by any other anion. For example, Br-HTC could be synthesized by calcining

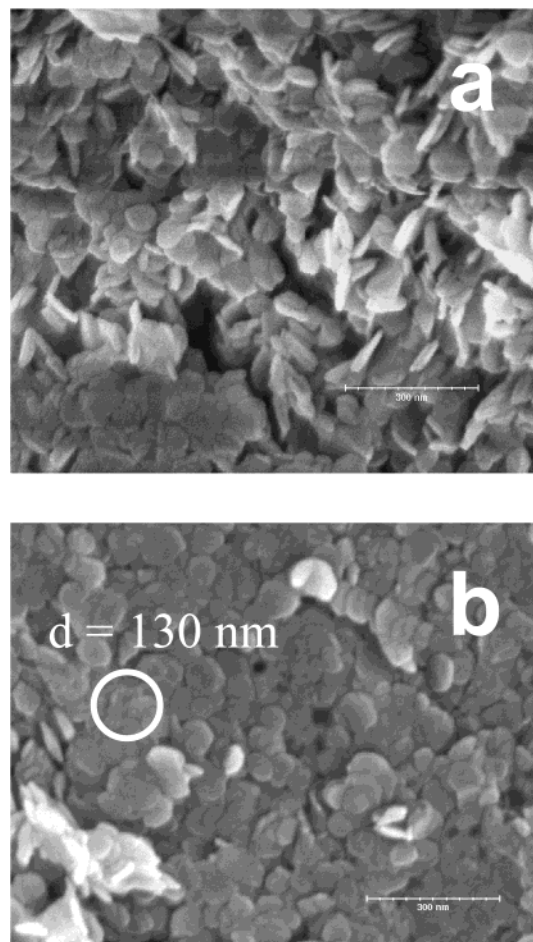


**Figure 2.** SEM images of Cl-HTC (a) and Cl/ $NO_3$ -HTC (b); the inserted white circle with  $d = 130$  nm illustrates the scale and average particle size.

$NO_3$ -HTC and dipping the amorphous Mg–Al–OH residue in NaBr solution.

**Hydrothermal.** The hydrothermal method produced powders of excellent crystallinity and high yields. Experiments carried out at temperatures ranging between 50 and 150 °C showed that the crystallinity improves with 12-hour treatments up to 90 °C, after which it remains virtually unchanged. In additional experiments the samples were treated at 90 °C for different periods of time ranging between 1 and 120 h. The results showed that the time and yield of well-crystallized products depend linearly on temperature — the higher the temperature, the shorter time of heating is necessary in order to get well-crystallized HTCs. The type of monovalent anion does not affect the general trend for the time, temperature, or crystallinity.

**Physical Characterization.** All preparations described above resulted in finely dispersed off-white powders. Typical SEM images of single-anion (A-HTC) and mixed (AA'-HTC) HTCs are shown in Figure 2. In both cases the crystallites had a uniform characteristic platelike shape and average diameter within the range 100–150 nm.

Surface area measurements showed a significant difference in the surface areas, depending on the type of the HTCs and the synthetic method used. The single-anion HTCs showed relatively small surface areas of about 2 m<sup>2</sup>/g, whereas the surface areas of the ion-

(21) Shannon, R. D. *Acta Crystallogr.* **1976**, A 32, 751.



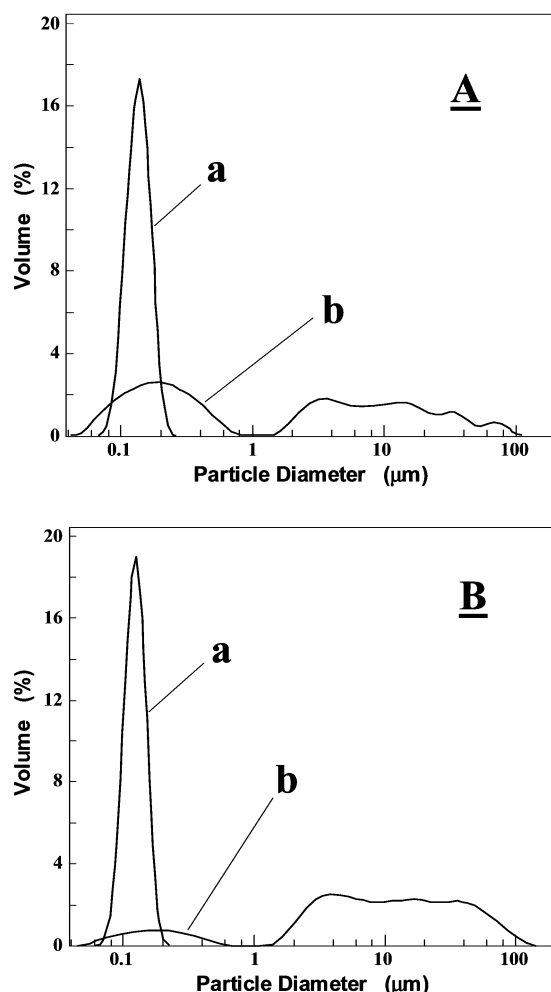


**Figure 3.** Particle size distribution in Cl-HTC (A) and Cl/NO<sub>3</sub>-HTC (B); (a) as-synthesized ("wet") and (b) dry samples.

exchanged double-anion AA'-HTCs were typically about 50 m<sup>2</sup>/g. For example, the surface area of the NO<sub>3</sub>-HTC synthesized by the hydrothermal method was 1.726(3) m<sup>2</sup>/g, but that of the mixed Cl/NO<sub>3</sub>-HTC was 45.6(2) m<sup>2</sup>/g. The difference in the values shows the variability in the primary particle packing (agglomerating) upon drying. The NO<sub>3</sub>-HTC sample packs better than the Cl/NO<sub>3</sub>-HTC material, which results in reducing its surface area and stronger aggregation.

Particle size distribution (PSD) measurements confirmed this observation; typical PSD curves of two different samples (A- and AA'-HTCs) are shown in Figure 3. The "wet" samples showed a relatively narrow PSD within the range 0.10–0.15 μm. The "dry" samples, on the other hand, showed much broader distribution. The partial volume of the 0.10–0.15 μm fraction significantly decreases and tends to broaden toward larger sizes. In the same time the particle size of the main fraction covers a wide range between 1 and 100 μm. This result is consistent with the surface area measurements and SEM observations. It confirms that upon drying the small particles (~0.1 μm) tend to stick together forming larger mechanical aggregates of up to 100 μm. The PSD for the "wet" samples is also consistent with the characterization of A-HTCs prepared by other methods.<sup>1–2,14,17</sup>

**XRD Studies.** X-ray powder diffraction was used to study the crystallinity, cell parameters, and interlayer separation *L* (Mg/Al/OH–Mg/Al/OH) of the series of

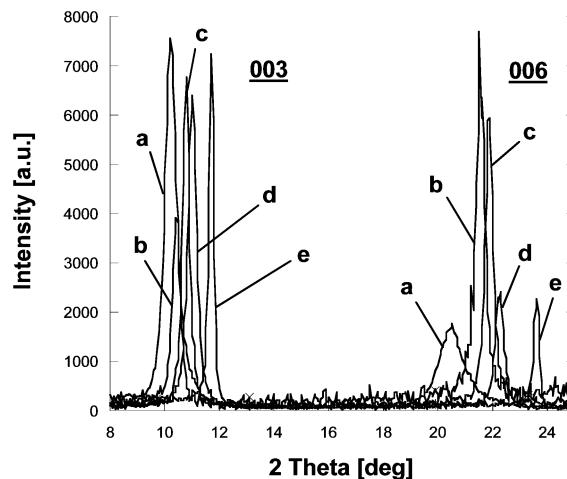


**Figure 4.** Typical low-angle XRD patterns of NO<sub>3</sub>-HTC (a), I-HTC (b), Br-HTC (c), Cl-HTC (d), and CO<sub>3</sub>-HTC (e).

single-anion A-HTCs (A = Cl<sup>−</sup>, Br<sup>−</sup>, I<sup>−</sup>, NO<sub>3</sub><sup>−</sup>, and CO<sub>3</sub><sup>−</sup>) as a function of the ionic radii of the anions involved.<sup>21</sup> Typical low-angle XRD spectra showing the strongest and most characteristic 003 and 006 reflections of the pure A-HTCs are presented in Figure 4. All preparations resulted in single-phase HTCs of good crystallinity with a very strong layer orientation perpendicular to the crystallographic *c*-axis.

A careful examination and comparison of the XRD spectra revealed a detail about the overall HTC layered structure and the possibilities of controlled anionic substitution. The structure presented in Figure 1 shows that the (003) plane contains the Mg/Al/OH layers, while the (006) one contains exclusively the anionic layers. Because the preparations in our A-HTCs series differ only by the type of the occluded anions, one would expect the XRD spectra to differ mostly in terms of the intensity of the related 006 reflections. Indeed, this is exactly what was observed in our experimental XRD spectra—the intensity of the 003 reflections remain virtually unchanged while the intensity of the 006 ones changes as a function of the electron density associated with the accommodated anion.

As expected, our XRD studies also showed that the *c*<sub>0</sub>-cell parameter and the interlayer separation *L* depend almost linearly on the anionic radii (Figure 5). The case of NO<sub>3</sub>-HTC was of particular interest because of the specific geometry of the NO<sub>3</sub><sup>−</sup> anion. Structural analysis showed that there are three distinct characteristic orientations of the NO<sub>3</sub> group that could affect the interlayer separation *L* and thus the *c*<sub>0</sub>-cell parameters as illustrated in Figure 6. As there are no known examples of NO<sub>3</sub>-HTCs with "flat" NO<sub>3</sub> groups, i.e., oriented with their planes parallel to the MOH layers,<sup>22</sup> the experimental values for CO<sub>3</sub>-HTC where the CO<sub>3</sub> anions are in this particular orientation<sup>2</sup> were used in our analysis. Comparing the ionic radii of N<sup>5+</sup>, C<sup>4+</sup>, and O<sup>2−</sup>, it is evident that the "thickness" of a "flat" triangular XO<sub>3</sub> group is determined by the size of the biggest atom, in this case O<sup>2−</sup>.<sup>21</sup> Therefore, in our calculations we assumed that the interlayer separation in CO<sub>3</sub>-HTC is the same as that in NO<sub>3</sub>-HTC with "flat" NO<sub>3</sub> groups (Figure 6a). The XRD analysis showed that

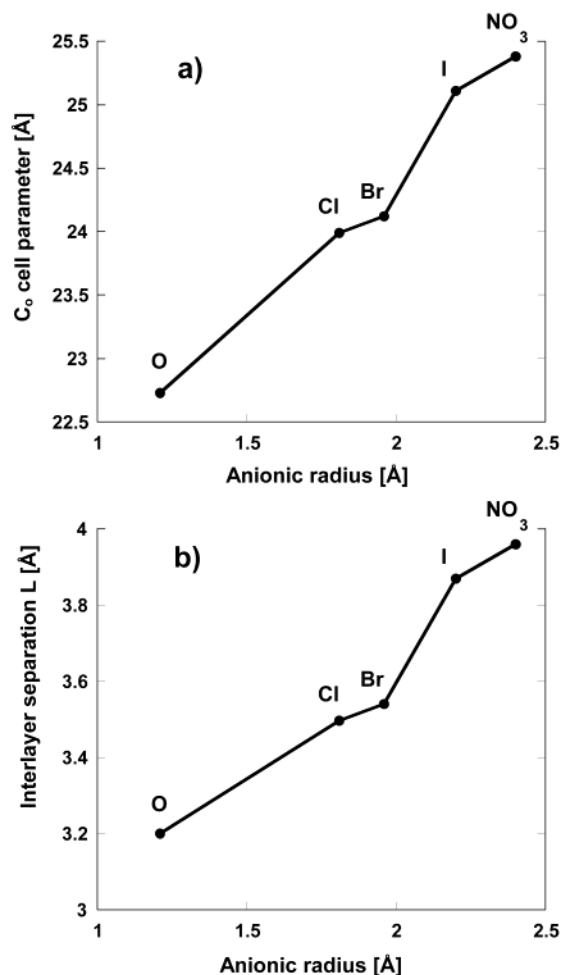


**Figure 5.** Changes of the  $c_0$ -cell parameter (top) and (Mg/Al/OH)-(Mg/Al/OH) interlayer separation  $L$  (bottom) as a function of the anionic radii in A-HTCs.

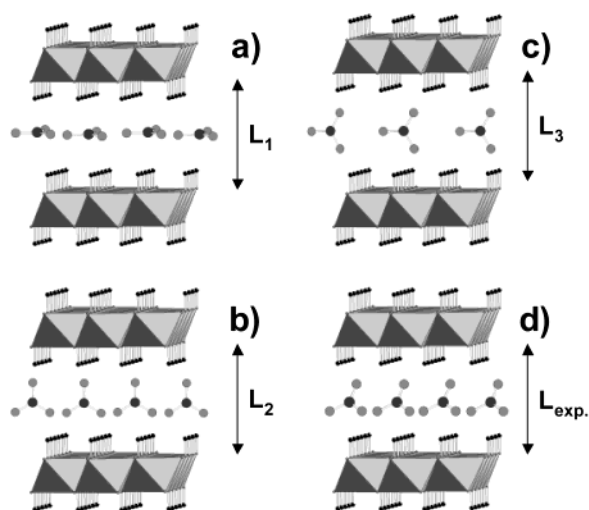


**Figure 6.** Different characteristic orientations of the  $\text{NO}_3$  group in  $\text{NO}_3$ -HTC.  $L_1 = 3.20$ ,  $L_2 = 4.74$ ,  $L_3 = 5.11$ , and  $L_{\text{exp}} = 3.96$  Å.

in our  $\text{NO}_3$ -HTC preparation the interlayer separation  $L$  is 3.96 Å. This indicates that the actual orientation of the  $\text{NO}_3$  groups is in a "tilted" configuration as shown in Figure 6d, i.e., between the "flat" and the "upright" orientations shown in Figure 6a and b.

Our next step was to study the same correlations in mixed AA'-HTCs. Here again, preliminary consider-

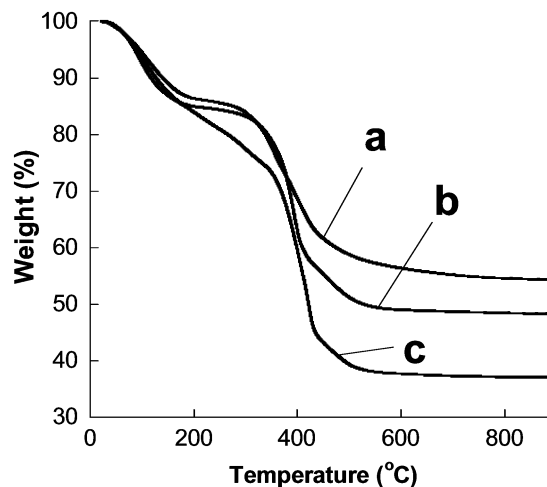


**Figure 7.** TGA curves of Cl-HTC (a), Cl/ $\text{NO}_3$ -HTC (b), and  $\text{NO}_3$ -HTC (c).

ations indicated that the changes of  $c_0$  and  $L$  would depend mostly on the size and relative amount of the occluded anions. Our XRD experiments, however, showed that there is no linear correlation. Because  $L$  illustrates better the expansion or shrinkage of the structure (i.e., reflects the changes of the separation between adjacent Mg/Al/OH layers as a function of the anionic content) the corresponding experimental values will be discussed next, together with the compositional and ion exchange characteristics of the mixed HTCs.

**Thermogravimetric Studies.** TGA analysis showed that the thermal decomposition of all HTCs takes place in two distinct steps (typical TGA curves are shown in Figure 7). The first step takes place between room temperature and 250 °C and corresponds to loss of the water molecules located between the Mg/Al/OH layers. At this stage the samples still preserve their crystallinity and HTC layered structure as seen by XRD analyses. The second step takes place between 250 and 500 °C and corresponds to a gradual loss of the anions and more water molecules resulting from condensation of the OH groups from the Mg/Al/OH layers, most probably as the corresponding HA/ $\text{H}_2\text{O}$  acids. This was confirmed by additional TGA experiments carried out in air flux passing through the heating chamber and through a flask filled with 50 mL of DI water. The pH values of the water in the trap dropped significantly after heating between 250 and 500 °C, for example from a pH of 7.0 down to a pH of 3.5 for 1 g of Cl/ $\text{NO}_3$ -HTC sample. At this stage the overall HTC structure collapses and the samples become amorphous powders (XRD data) of nominal composition  $\text{Mg}_6\text{Al}_2(\text{OH})_{18}$ . At the final stage of decomposition ( $T \geq 500$  °C) the samples lose the remaining OH/ $\text{H}_2\text{O}$  and correspond to a mixture of MgO and  $\text{Al}_2\text{O}_3$  (XRD data). The theoretical calculations describing the whole process compared well with our experimental data, for example in the case of Cl-HTC (Figure 7a): Step I,  $\text{Mg}_6\text{Al}_2(\text{OH})_{16}\text{Cl}_2 \cdot 5\text{H}_2\text{O} - 5\text{H}_2\text{O}$  (Calc. Wt. Loss = 14.20%); Step II,  $\text{Mg}_6\text{Al}_2(\text{OH})_{16}\text{Cl}_2 - 2\text{HCl} - 7\text{H}_2\text{O} \rightarrow 6\text{MgO} + \text{Al}_2\text{O}_3$  (Calc. Total Wt. Loss = 45.66%). Our experimental TGA data for single-anion HTCs also compare well with those of similar reported studies.<sup>1,2,17</sup>

**FTIR.** This analytical technique provided a fast, easy, and reliable method for a qualitative evaluation (yes/

**Table 1. A'/A Ratios in the A,A'-HTCs Formed after Ion Exchange (A-HTC)<sub>solid</sub>/(NaA')<sub>soln</sub>**

A-HTC	A'/A (A' from (NaA') <sub>soln</sub> )			
	Cl	Br	I	NO <sub>3</sub>
Cl		5.62	2.50	3.40
Br	1.64		3.69	1.22
I	40.00	11.30		4.42
NO <sub>3</sub>	4.75	21.40	3.09	

**Table 2. Final Cationic Ratios (%) in the Resulting Solid HTCs after Ion Exchange (A<sub>i</sub>-HTC)<sub>solid</sub>/Σ(NaA<sub>j</sub>)<sub>soln</sub>**

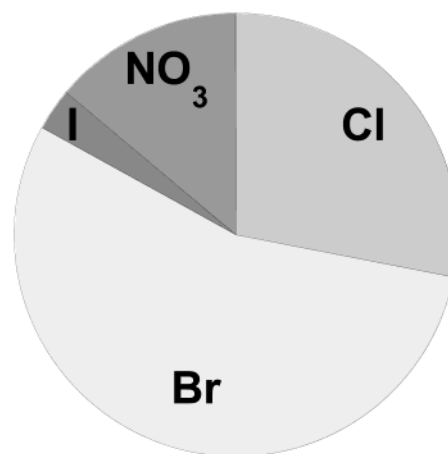
(A <sub>i</sub> -HTC) <sub>solid</sub>	final A <sub>i</sub> A <sub>j</sub> ' (%)			
	Cl	Br	I	NO <sub>3</sub>
Cl	29	54	7	10
Br	27	35	15	23
I	25	44	8	23
NO <sub>3</sub>	31	53	7	9

no tests) and comparison of the relative degree of incorporation of NO<sub>3</sub> in the NO<sub>3</sub><sup>-</sup> and NO<sub>3</sub>/A-HTCs prepared by different methods. It also allowed, and was used for, monitoring the possible undesirable formation of CO<sub>3</sub>-HTC and CO<sub>3</sub>/A-HTCs due to absorption of CO<sub>2</sub> from the air.

**Ion Exchange.** Results of the simple A' → A exchange of (A-HTC)<sub>solid</sub>/(A')<sub>soln</sub> (A, A' = Cl, Br, I, and NO<sub>3</sub>) systems are summarized in Table 1. In all cases a measurable A' → A ion exchange takes place; the A'/A ratios in the so-formed AA'-HTCs ranged between 1.2 and 40. The solid Cl- and NO<sub>3</sub>-HTCs show highest preference for exchange with Br<sup>-</sup> from solution, whereas Br- and I-HTCs show highest preference for I<sup>-</sup> and Cl<sup>-</sup> from solutions, respectively.

Preliminary theoretical analyses predicted that the dominant anion size would determine the interlayer separation *L* in the resulting AA'-HTCs after the ion exchange. However, our XRD data indicated that this is not always valid and predictable. For example, the resulting *L* values for the series (NO<sub>3</sub>-HTC)<sub>solid</sub>/(NaA')<sub>soln</sub> (A' = Cl and Br) changed from 3.96 Å (NO<sub>3</sub>-HTC) to 3.48 and 3.55 Å, respectively, which correspond to pure Cl- and Br-HTCs (Figure 5b). A comparison of these values with that of the NO<sub>3</sub> group in different orientations also shows that in both cases the remaining NO<sub>3</sub> groups should be in an almost "flat" configuration (Figure 6). In the (NO<sub>3</sub>-HTC)<sub>solid</sub>/(NaI)<sub>soln</sub> system, however, the initial *L* value of 3.96 Å remained virtually unchanged even after significant I<sup>-</sup> → NO<sub>3</sub><sup>-</sup> ion exchange had taken place (final I/NO<sub>3</sub> = 3:1, Table 1). This result indicates that in this particular case the "tilted" NO<sub>3</sub><sup>-</sup> anions of the original HTC most probably act like pillars and the I<sup>-</sup> anion exchange does not affect the interlayer separation. Similar anomalies have been also observed in some of the other systems, for example in the (Cl-HTC)<sub>solid</sub>/(NaA')<sub>soln</sub> systems where in all cases the resulting *L* values correspond to that of the pure Cl-HTC although significant ion exchange had taken place (Table 1).

The experimental ion exchange preferences when all four anions were present are summarized in Table 2. All starting A-HTCs showed highest selectivity toward Br<sup>-</sup>. In all cases, the order of preference, i.e., the amount of anions incorporated in the solid product after the ion exchange, was Br<sup>-</sup> > Cl<sup>-</sup> > NO<sub>3</sub><sup>-</sup> > I<sup>-</sup>. As in the case of the (Cl-HTC)<sub>solid</sub>/(NaA')<sub>soln</sub> systems described above,

**Figure 8.** Final anionic content in (Cl/Br/I/NO<sub>3</sub>)-HTC made by one-pot synthesis: Br<sup>-</sup> = 55%, Cl<sup>-</sup> = 28%, NO<sub>3</sub><sup>-</sup> = 14%, and I<sup>-</sup> = 3%.**Table 3. A'/A Ratios in the A,A'-HTCs Formed after One-Pot Syntheses**

A'/Cl ratio in A,A'-HTCs			
A'/Cl ratio (solution)	Br	I	NO <sub>3</sub>
1:3	0.33	0.06	0.13
1:1	2.29	1.21	0.74
A'/NO <sub>3</sub> ratio in A,A'-HTCs			
A'/NO <sub>3</sub> ratio (solution)	Cl	Br	I
1:3	0.03	0.47	0.27
1:1	1.40	8.86	2.17

the Cl<sup>-</sup> anions which present at levels of 25% or more in all exchanged HTCs determine the interlayer separation *L*.

**One-Pot Syntheses.** Results of the binary (A + A') hydrothermal reactions are summarized in Table 3. In all cases double AA'-HTCs have been formed. Our results confirmed the general trend observed for the above two series. Both ClA'- and NO<sub>3</sub>A'-HTCs showed highest preference to incorporate Br<sup>-</sup>. Our results also showed that it is possible to control the degree of incorporation by controlling the starting A'/A ratio: the higher the ratio, the higher the degree of incorporation of A' in the resulting AA'-HTC. In all ClA'-HTCs the interlayer separations *L* was determined by the Cl<sup>-</sup> anions. In the case of NO<sub>3</sub>A'-HTCs when the starting NO<sub>3</sub>/A' ratio was 1:1, the *L* values of the final products were determined by the corresponding A<sup>-</sup> anions. When NO<sub>3</sub>/A' = 3:1 the *L* values were equal to that of the pure NO<sub>3</sub>-HTC with NO<sub>3</sub><sup>-</sup> in "tilted" configuration as shown in Figure 6d. There seems to be a certain limit of the NO<sub>3</sub> content below which these could not serve as pillars any more. Furthermore, the relatively high NO<sub>3</sub> content in the NO<sub>3</sub>/A' = 1:1 samples indicates that most probably the resulting *L* values are also strongly affected by the mechanism and kinetics of the process of AA'-HTC formation from solution.

The results of the one-pot hydrothermal syntheses when all four anions (Cl<sup>-</sup>, Br<sup>-</sup>, I<sup>-</sup>, and NO<sub>3</sub><sup>-</sup>) are present are summarized in Figure 8. As one can see, the previously described tendency holds here as well: the order of incorporation preference is also Br<sup>-</sup> > Cl<sup>-</sup> > NO<sub>3</sub><sup>-</sup> > I<sup>-</sup>. Here again, the smallest Cl<sup>-</sup> anion presenting as 28% of the total anionic content (compared to the

bigger  $\text{Br}^-$  with twice the concentration, 55%) determines the  $L$  value of the final (Br/Cl/ $\text{NO}_3^-$ /I)-HTC.

### Conclusions

We present here a comprehensive study of the monovalent anion exchange preferences of hydrotalcite clays, independent of the method of synthesis or anion occlusion. The physical (morphology, surface area, and particle size distribution), structural (cell parameters, interlayer separation) and chemical (composition, ion-exchange capacity) characteristics and properties of the HTCs have been studied as a function of the synthetic methods and anions used. All three synthetic methods used — ion exchange (IE), hydrothermal (HT), and “memory effect” (ME) — resulted in HTCs of good crystallinity and uniform particle size of about  $0.1\ \mu\text{m}$ . Upon drying, the particles tend to aggregate in larger agglomerates of up to  $100\ \mu\text{m}$ .

Single-anion HTCs (A-HTCs) could be synthesized only by one-pot reactions using HT or ME methods. Consecutive ion exchange experiments showed that there was no complete substitution of one anion for another. When a second ( $\text{A}'$ ) or all four ( $\text{Cl}^-$ ,  $\text{Br}^-$ ,  $\text{I}^-$ , and  $\text{NO}_3^-$ ) anions were present in the system, all

A-HTCs showed highest selectivity for ion exchange with  $\text{Br}^-$ . For all A-HTCs, the order of preference for ion exchange was  $\text{Br}^- > \text{Cl}^- > \text{NO}_3^- > \text{I}^-$ .

Mixed ( $\text{AA}'$ -HTCs) could be prepared by all three methods. When using one-pot syntheses (HT and ME), the final A/ $\text{A}'$  ratio is proportional to, and could be controlled by, the starting A/ $\text{A}'$  ratio — the higher the ratio, the higher the A-anion incorporation into the final  $\text{AA}'$ -HTCs. When using equimolar starting NaA solutions, the order of anion incorporation preference was  $\text{Br}^- > \text{Cl}^- > \text{NO}_3^- > \text{I}^-$ . Ongoing research in this area includes comparison of preferential monovalent versus divalent anion incorporation into HTCs, and the effects of HTC-“framework” metal doping on anion selectivity.

**Acknowledgment.** We thank Diana Sipola for the particle size distribution, surface area determination, and SEM images. Sandia is a multiprogram laboratory operated by Sandia Corporation, a Lockheed Martin Company, for the United States Department of Energy's National Nuclear Security Administration under contract DE-AC04-94AL85000.

CM034231R